Electronic Supplementary Material (ESI) for RSC Advances.

Supportting Information

Natural Sliced Wood Veneer as a Universal Porous Lightweight Substrate for Supercapacitor Electrode Materials

Shaoyi Lyu,[a]* Yanping Chen,[a,c] Shenjie Han,[a] Limin Guo,[a] Na Yang[a] and Siqun Wang[b,a]*

[a] Research Institute of Wood Industry, Chinese Academy of Forestry, Beijing 100091, China.
[b] Center for Renewable Carbon, University of Tennessee, Knoxville, Tennessee, 37996, USA.
[c] Beijing Engineering Research Center of Cellulose and Its Derivatives, School of Materials Science and Engineering, Beijing Institute of Technology, Beijing 100081, China.

*Author for correspondence. Email: lvsy@caf.ac.cn (S. Lyu), swang@utk.edu (S. Wang).

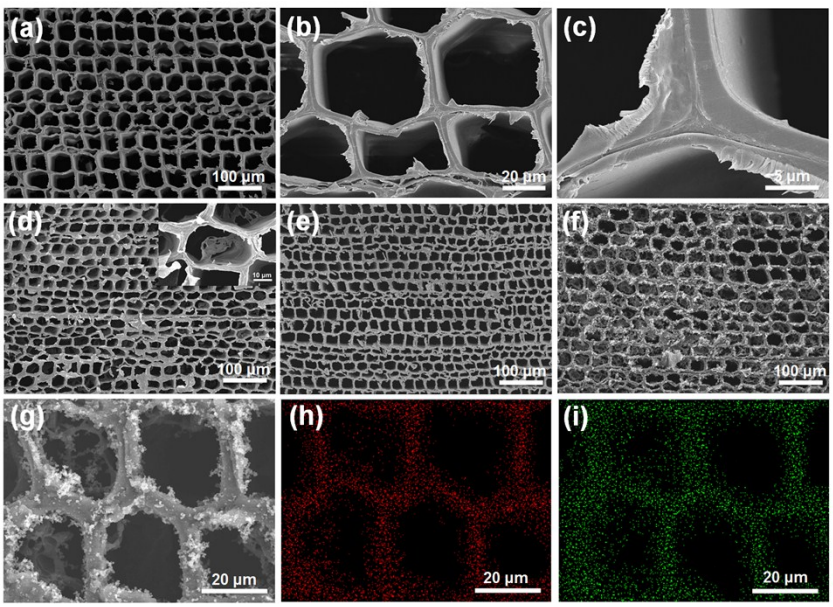

Fig. S1 (a-c) Surface morphology SEM images of natural wood at different scales. Surface morphology SEM images of (d) RGO wood, (e) PANI/RGO wood and (f) PPy/RGO wood at a small magnification. The inset of (d) shows an enlarged scale of RGO wood. (g–i) SEM/EDS image of the PPy/RGO wood. (h and i) Corresponding elemental mapping images of (h) N, and (i) C.

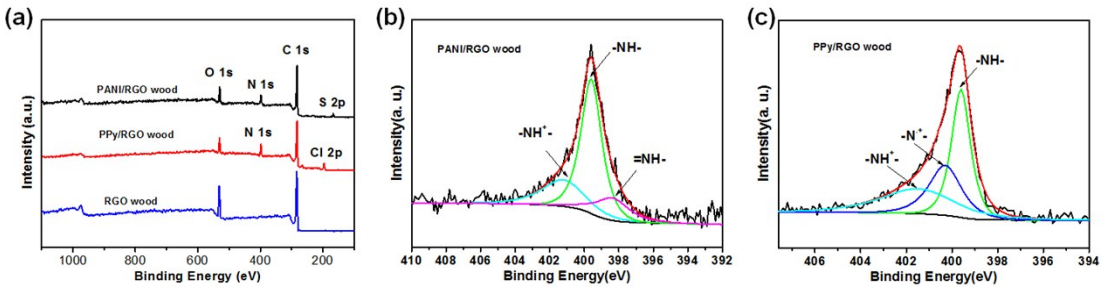

Fig. S2. (a) XPS wide-region scan spectrum of the PANI/RGO wood, PPy/RGO wood and RGO wood. High-resolution XPS N 1s spectrum of the (b) PANI/RGO wood and (c) PPy/RGO wood.

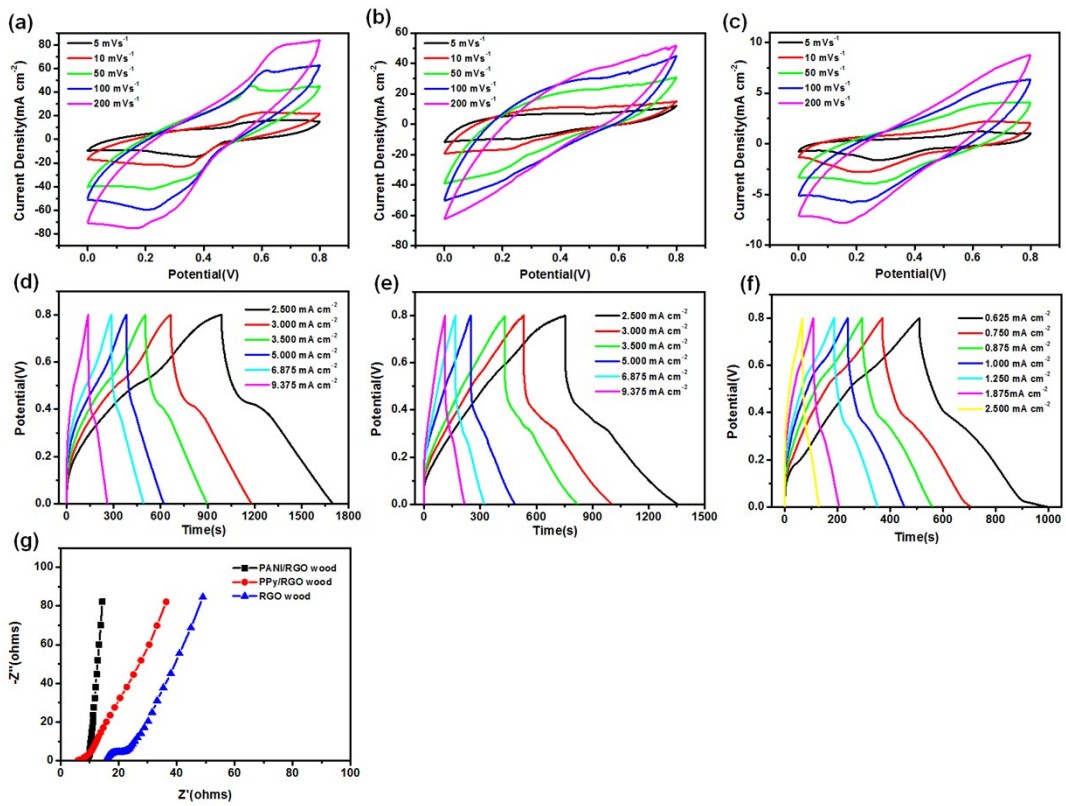

Fig. S3. CV curves of the (a) PANI/RGO wood, (a) PPy/RGO wood and (c) RGO wood electrodes at different sweep rates. GCD curves of (d) PANI/RGO wood, (e) PPy/RGO wood and (f) RGO wood electrodes at different current densities. (g) Nyquist plots of three wood electrodes. The electrochemical performances of three wood electrodes here were under three-electrode tests.

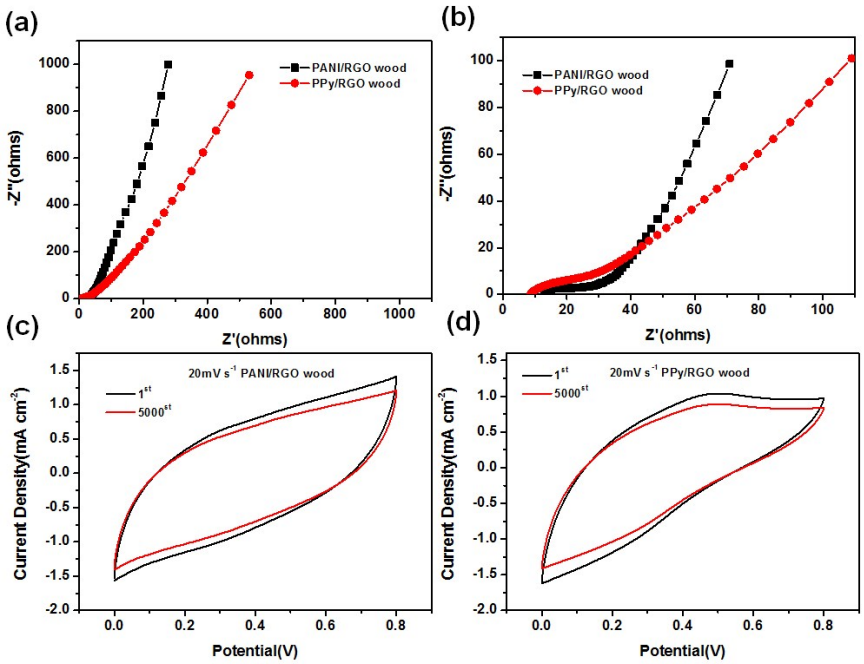

Fig. S4. (a) Nyquist plots of PANI/RGO wood and PPy/RGO wood electrodes assembled supercapacitor. (b) The enlarged scale of (a) at high frequency. CV curves of (c) PANI/RGO wood and (d) PPy/RGO wood electrodes assembled supercapacitor for cycling stability test.

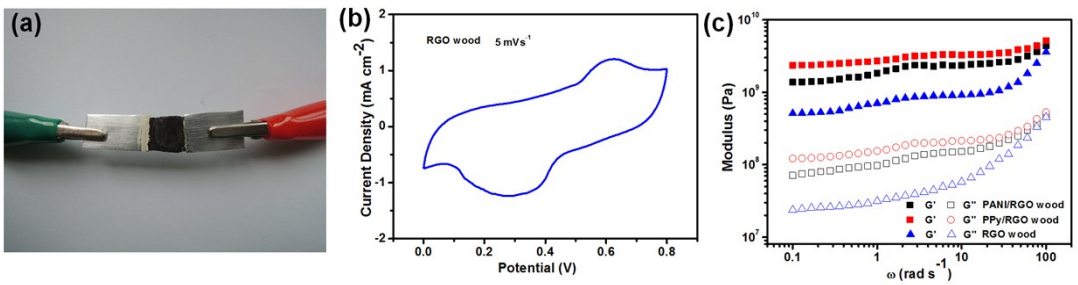

Fig. S5. (a) The assembled all-solid-state supercapacitor device. (b) CV curve of the RGO wood electrode at a sweep rate of $5mVs^{-1}$. (c) Dynamic mechanical properties of PANI/RGO, PPy/RGO and RGO wood electrodes.

Tab. S1. The electrochemical performances of various electrodes.

Scaffolds	Active material	Current density	Specific capacitance	References
free-standing	graphene/polyanilin e	1 A g^{-1} (3-electrode) 1 A g^{-1} (2-electrode)	777 F g^{-1}(3-electrode) 665 F g^{-1}(2-electrode)	S1
free-standing	polyaniline/N-doped porous carbon	1 A g^{-1} (3-electrode)	755 F g^{-1}(3-electrode)	S2
free-standing	polyaniline/activated wood derived carbon	2 A g^{-1} (3-electrode)	372 F g^{-1}(3-electrode)	S3
cotton fabric	polypyrrole/reduced graphene oxide	0.6 mA cm^{-2}(3-electrode)	336 F g^{-1}(3-electrode)	S4
paper	graphite/polyaniline	0.5 mA cm^{-2} (3-electrode)	355.6 mF cm^{-2} (3-electrode)	S5
free-standing	carbon nanotube/polyaniline	1 mA cm^{-2}(3-electrode) 1 mA cm^{-2}(2-electrode)	680 mF cm^{-2}(3-electrode) 184.6 mF cm^{-2}(2-electrode)	S6
wood	polyaniline/reduced graphene oxide	2.5 mA cm^{-2}(3-electrode)	931.92 F g^{-1}(3-electrode) 298.52 F g^{-1}(2-electrode)	This work
	polypyrrole/reduced graphene oxide	0.50 mA cm^{-2}(2-electrode)	848.01 F g^{-1}(3-electrode) 258.82 F g^{-1}(2-electrode)	

Supplementary Reference

S1. K. Li, J. Liu, Y. Huang, F. Bu and Y. Xu, *J. Mater. Chem. A*, 2017, **5**. 5466-5474

S2. S. N. Guo, H. K. Shen, Z. F. Tie, S. Zhu, P. H. Shi, J. C. Fan, Q. J. Xu and Y. L. Min, *J. Power Sources*, 2017, **359**. 285-294

S3. D. Liu, S. Yu, Y. Shen, H. Chen, Z. Shen, S. Zhao, S. Fu, Y. Yu and B. Bao, *Ind. Eng. Chem. Res.*, 2015, **54**. 12570-12579

S4. J. Xu, D. Wang, Y. Yuan, W. Wei, L. Duan, L. Wang, H. Bao and W. Xu, *Org. Electron.*, 2015, **24**, 153-159.

S5. B. Yao, L. Yuan, X. Xiao, J. Zhang, Y. Qi, J. Zhou, J. Zhou, B. Hu and W. Chen, *Nano Energy*, 2013, **2**, 1071-1078.

S6. S. Zeng, H. Chen, F. Cai, Y. Kang, M. Chen and Q. Li, *J. Mater. Chem. A,* 2015, **3**, 23864-23870.